

## Modeling of polymer/clay nanocomposites by an iterative micromechanical approach

A. MOHYEDDIN, A. FEREDOON

*Department of Mechanical Engineering  
Semnan University  
Semnan, 35131-19111, Iran  
e-mail: a\_mohyeddin@sun.semnan.ac.ir*

AN ITERATIVE MICROMECHANICAL METHOD is presented in order to predict the elastic constants of composites and nanocomposites including arbitrarily oriented reinforcement particles. The proposed method is capable of introducing into the matrix any kind of heterogeneity based on its dimension, orientation, mechanical properties and volume fraction. The efficiency and convergence of solution method is studied by computing the elasticity tensor of a unidirectional particulate composite. It is then applied to model the elastic behavior of nylon-6/clay nanocomposite with taking into consideration the probability distribution of aspect ratio and orientation of effective particles. The results are validated by comparison with available experimental data.

**Key words:** polymer/clay nanocomposites, elastic properties, micromechanical modeling, iterative method, probability density function.

Copyright © 2012 by IPPT PAN

### 1. Introduction

EVER-INCREASING INDUSTRIAL DEMANDS for new materials withstanding extreme operating conditions, e.g., high temperature, aggressive environment, impact, etc., lead to a gradual replacement of conventional metallics with synthetic composite materials with increasing complexity in micro-structural and morphological properties. Most of these composites are polydisperse materials containing various geometric or thermo-mechanical types of fillers. This is the case, for example, in syntactic foams made of hollow glass microspheres with various thicknesses embedded in a polymeric matrix, polymer/clay nanocomposites containing nanoparticles with different aspect ratios (geometric dispersion) or particulate composites, gathering the desired properties of two or more filling constituents (thermo-mechanical dispersion).

Numerical methods have become an effective homogenization tool in order to predict the behavior of such materials, as they allow to simulate microstructures similar to the real ones, under any type of loading, as well as taking into account the interactions between micro- and macro- levels [1–7]. Despite of effectiveness of

these numerical approaches, explicit micromechanical models remain attractive for their easy implementation and their capacities to test various parameters with the aim of optimizing their properties.

Most of the micromechanical models are based on the solution of an elliptical inclusion isolated in an infinite elastic matrix suggested by ESHELBY [8]. Thus, one can cite the generalized self-consistent model [9, 10], Mori–Tanaka model [11], the morphological approach [12, 13] or the differential scheme proposed by NORRIS [14] and ZIMMERMAN [15] based on an iterative procedure. Some of these approaches, which were initially proposed for monodisperse composites, have been generalized to take into account various behaviors of reinforcements. For example, BUDIANSKY [16] has extended the self-consistent model for composites with several families of spherical inclusions with different behaviors and PHAN-THIEN and PHAM [17] have generalized the differential scheme to model multiphase mediums. BARDELLA and GENNA [18] have suggested also a multiphase homogenization method from morphological model applied to syntactic foams with different sizes of hollow microspheres.

The enhancement in mechanical properties of nanocomposites has inclined many authors to develop aforesaid micromechanical models for predicting the behavior of these materials. KOJIMA *et al.* [19] and SHELLEY *et al.* [20] used the rule of mixtures to estimate the elastic modulus of polyamide-6/clay nanocomposites. BRUNE and BICERANO [21] studied the effect of incomplete exfoliation and deviation of the platelets from perfect biaxial in-plane orientation on the compressive stiffness of nanocomposites using the Halpin–Tsai [22] equation. LUO and DANIEL [23] applied the Mori–Tanaka method to calculate the modulus of polymer/clay nanocomposites for various parametric variations related to material and geometric properties and microstructure/nanostructure morphology. ANOUKOU *et al.* [24] presented a self-consistent scheme based on the double-inclusion model to calculate the overall stiffness tensor of polymer-clay nanocomposites assuming randomly oriented reinforcements. Introducing the interaction between clay and matrix in their analysis, MESBAH *et al.* [25] assumed the presence of an interphase between the two phases (polyamide-6 and clay) and considered the interphase thickness as a characteristic length scale. They estimated the fraction of interphase region using the approach proposed by KOJIMA *et al.* [19] by means of DSC and DMA tests. They concluded that for randomly oriented particles, there is no major enhancement of the nanocomposite stiffness due to the morphological transition from intercalated to exfoliated state. ZAÏRI *et al.* [26] used the same formulation to predict the elastic-plastic behavior of nylon-6/clay nanocomposites. ANTHOULIS and KONTOU [27] combined Mori–Tanaka’s [11] theory with the self-consistent model of BUDIANSKY and WU [28] to formulate the elastic-plastic response of epoxy/clay nanocomposites, formerly tested by LUO and DANIEL [23].

Although explicit micromechanical methods are in good agreement for slightly reinforced, weakly contrasted or dispersed composites, they can significantly differ for highly reinforced or polydisperse composites. Furthermore, their applications are limited to composites with random [23–29] or unidirectional [23, 25] filler orientations. To overcome these shortcomings, ZOUARI *et al.* [30] proposed an iterative process of homogenization in order to characterize the mechanical behavior of composites highly reinforced by spherical inclusions of various types and dimensions. But their method can only be useful for isotropic composites containing spherical inclusions.

Regarding these remarks, the aim of this work is to extend the foregoing iterative approach in order to predict the behavior of more general particulate composites, specifically polymer/clay nanocomposites.

Contrary to what may appear at first glance, the proposed method is preferred over the conventional differential method, because it is capable of predicting the behavior of particulate composites with any degree of heterogeneity, material symmetry and reinforcement. Furthermore, it can handle any distribution function for physical and structural parameters of composite, including level of filler-matrix interfacial bonding, aspect ratio and orientation of reinforcement particles.

This paper is organized as follow: Section 2 briefly discusses the general process of micromechanical iterative approach. In Section 3, the implementation is validated and the convergence of the process is analyzed. Section 4 presents iterative modeling procedure of intercalated polymer/clay nanocomposites assuming nanoparticles as Eshelby's inclusions with effective mechanical properties. In Section 5, available experimental results for a fully exfoliated nylon-6/clay nanocomposite are presented to assess results of proposed method. Final section is dedicated to discussion about the results and conclusion.

## 2. Iterative method for polydisperse composite materials

Following a similar principle to the differential scheme introduced by NORRIS [14] and iterative homogenization process applied by ZOUARI *et al.* [30], the proposed iterative approach consists of gradually introducing filler constituents of a polydisperse composite with  $m$  types of heterogeneities into its matrix. To this end, firstly each filler type is divided into  $n$  equal parts, each with volume fraction  $V_i/n$ . At the initial step, the first part of the first filler type is added to the matrix. Then, the equivalent elasticity tensor of this first virtual medium is obtained by any micromechanical homogenization method such as Eshelby, Mori–Tanaka, self-consistent [31], HASHIN [32] and HALPIN– TSAI [22]. This homogeneous medium constitutes the matrix of the intermediate composite which is again homogenized at the next step. This process is reiterated  $m$  times by

adding the first element of each filler type at each iteration. The overall procedure is then repeated  $n$  times for  $j$ th elements of all filler types until the final volume fraction of filler is reached. The computed elasticity tensor at this step results in the effective elasticity tensor of the polydisperse composite.

The filler volume fraction, relevant to iteration  $j$  could be obtained from in

$$(2.1) \quad V_j = \frac{V_f}{jV_f + mn(1 - V_f)}, \quad j = 1, 2, \dots, mn.$$

Equation (2.1) is obtained for the case when all filler components have the same volume fraction.

The homogenization method applied in this study is based on the standard Mori–Tanaka approach with the following formulation [33]:

$$(2.2) \quad \begin{aligned} \bar{\mathbf{L}} &= (V_m \mathbf{L}_m + V_f \mathbf{L}_f \mathbf{T}_f)(V_m \mathbf{I} + V_f \mathbf{T}_f)^{-1}, \\ \mathbf{T}_f &= [\mathbf{I} + \mathbf{S} \mathbf{L}_m^{-1} (\mathbf{L}_f - \mathbf{L}_m)]^{-1}, \end{aligned}$$

where  $\mathbf{I}$  is the fourth-order identity matrix,  $\mathbf{S}$  is the Eshelby tensor, and  $V_m$  and  $V_f$  are matrix and filler volume fractions, respectively.  $\bar{\mathbf{L}}$ ,  $\mathbf{L}_m$  and  $\mathbf{L}_f$  are elasticity tensors for composite, matrix and filler, respectively.

As stated in Eqs. (2.2), the effective elasticity tensor at  $j$ th iteration will be obtained as

$$(2.3) \quad \begin{aligned} \bar{\mathbf{L}}^{(j+1)} &= [(1 - V_j) \bar{\mathbf{L}}^{(j)} + V_j \mathbf{L}_f^{(j)} \mathbf{T}_f^{(j)}] [(1 - V_j) \mathbf{I} + V_j \mathbf{T}_f^{(j)}]^{-1}, \\ \mathbf{T}_f^{(j)} &= [\mathbf{I} + \mathbf{S}^{(j)} (\bar{\mathbf{L}}^{(j)})^{-1} (\mathbf{L}_f^{(j)} - \bar{\mathbf{L}}^{(j)})]^{-1}, \quad j = 1, 2, \dots, mn, \end{aligned}$$

where  $\bar{\mathbf{L}}^{(1)} = \mathbf{L}_m$  and  $\bar{\mathbf{L}}^{(j)}$  and  $\bar{\mathbf{L}}^{(j+1)}$  are elasticity tensors of intermediate matrix corresponding to  $j$ th and  $(j + 1)$ th iterations.

It is noticeable that the coordinate systems (CS) used for computation of Eshelby's tensor and elasticity tensors of matrix and inclusion should be the same. To meet this condition, the CS attached to the inclusion is considered as the reference CS at each iteration. Thus, variation in direction of inclusion at each iteration requires transformation of matrix elasticity tensor obtained in previous step. The flowchart of this iterative procedure is shown in Fig. 1.

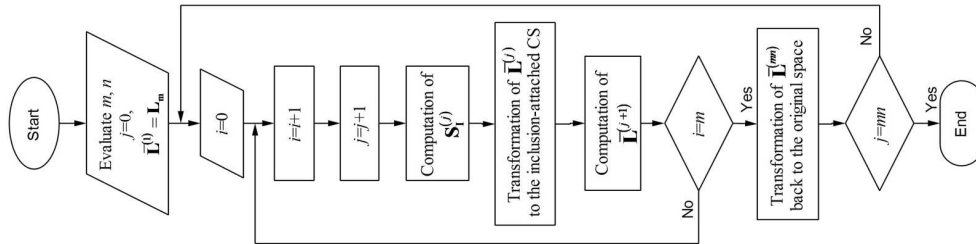


FIG. 1. Flowchart of micromechanical iterative process.

### 3. Implementation and convergence study of iterative process

#### 3.1. Modeling of monodisperse composites

ZOUARI *et al.* [30] applied the same approach for the simple case of monodisperse composite with identical spherical reinforcements. They coupled the iterative process with some micromechanical methods including strain (DA-strain) and stress approaches (DA-stress), Hashin's lower bound (Hashin-LB), Hashin's upper bound (Hashin-UB), Hashin's spherical composite (Hashin-SC), the three-phase method (3 phases), the differential schema (Diff) and the Mori–Tanaka approach (MT). The mechanical properties, used in this study, were  $E_m = 3.5$  GPa and  $E_f = 72$  GPa for Young's modulus, and  $\nu_m = 0.4$ ,  $\nu_f = 0.22$  for Poisson's ratio of matrix and filler, respectively. According to their findings, before applying the iterative process, all homogenization methods lead to different predictions, particularly in high degrees of reinforcement. But the coupling of the iterative homogenization process with various explicit methods leads to a unified prediction for the effective behavior after a sufficient number of iterations.

To validate our MAPLE code written for the present iterative procedure, the above problem is resolved by using the Mori–Tanaka method. In the continuation, the convergence trends of predicted Young's and shear moduli, are assessed in Figs. 2a and 2b, respectively. As it is shown, more iterations are required to get convergence at high volume fractions of filler.

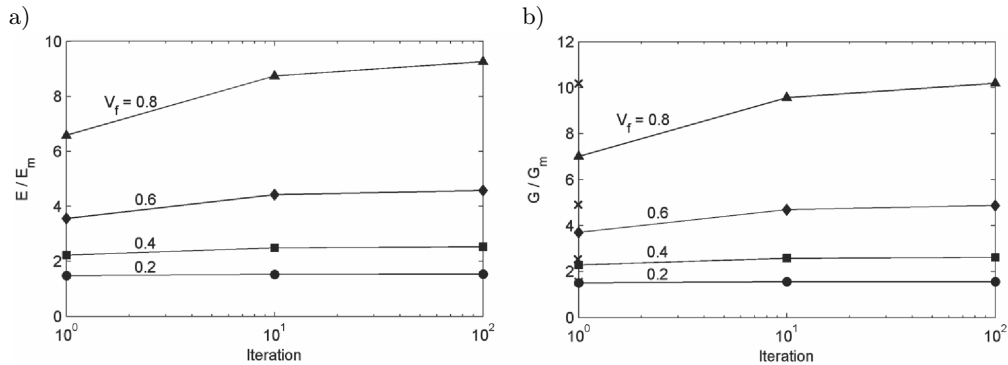


FIG. 2. Convergence trend of normalized effective properties for different values of filler volume fraction: a) Young's modulus, b) shear modulus. The reference data [30] for shear modulus are indicated by  $\times$ .

#### 3.2. Modeling of unidirectional composites

To study the effect of reinforcement volume fraction, aspect ratio and phase contrast on the predictions of both conventional (non-iterative) and iterative

Mori–Tanaka’s methods, a unidirectional particulate composite is considered in this section. The reinforcement particles are assumed as ellipsoidal inclusions with the following representative equation:

$$(3.1) \quad \left(\frac{x_1}{a_1}\right)^2 + \left(\frac{x_2}{a_2}\right)^2 + \left(\frac{x_3}{a_3}\right)^2 = 1, \quad a_1 = a_2,$$

where  $a_1$ ,  $a_2$  and  $a_3$  are the semi-axes of the ellipsoid.

Thus, the aspect ratio will be defined as  $\alpha = a_1/a_3$ . Assuming the value of 0.3 for Poisson’s ratio of both matrix and filler, the convergence trend of solution for different values of filler volume fraction  $V_f$ , filler aspect ratio  $\alpha$ , and elastic moduli ratio  $E_f/E_m$  are plotted in Figs. 3–5, respectively. It is concluded

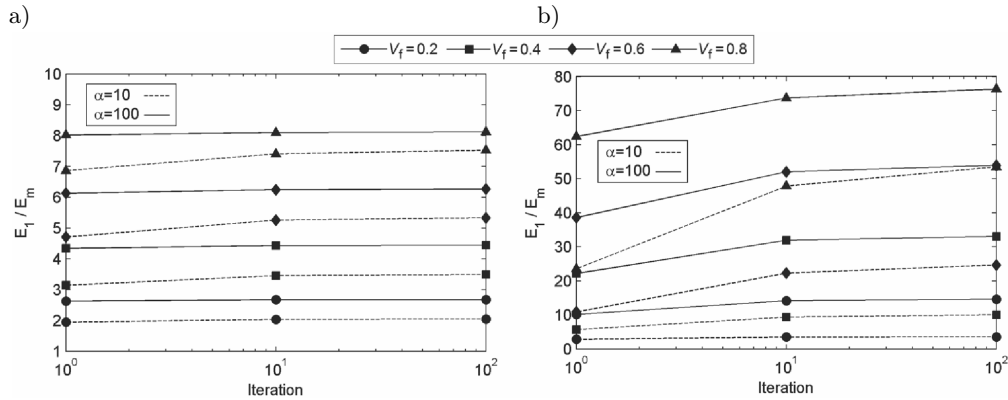


FIG. 3. Convergence trend of normalized effective longitudinal Young’s modulus for different values of filler volume fraction and aspect ratio: a)  $E_f/E_m = 10$ , b)  $E_f/E_m = 100$ .

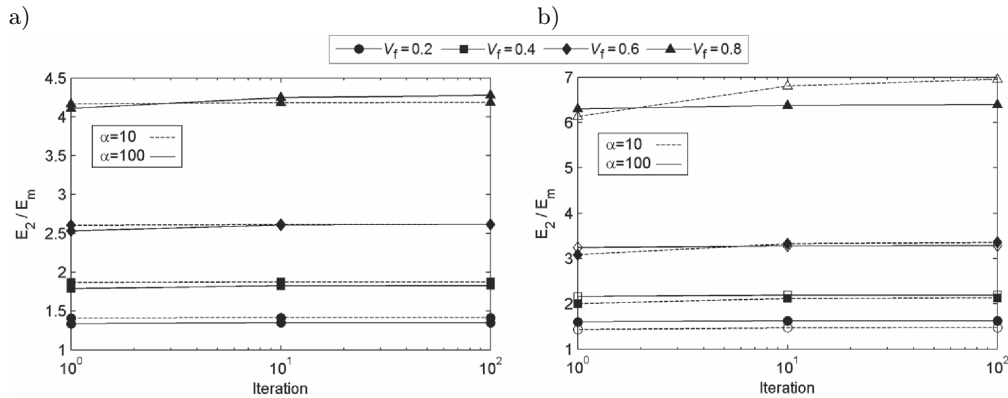


FIG. 4. Convergence trend of normalized effective lateral Young’s modulus for different values of filler volume fraction and aspect ratio: a)  $E_f/E_m = 10$ , b)  $E_f/E_m = 100$ .

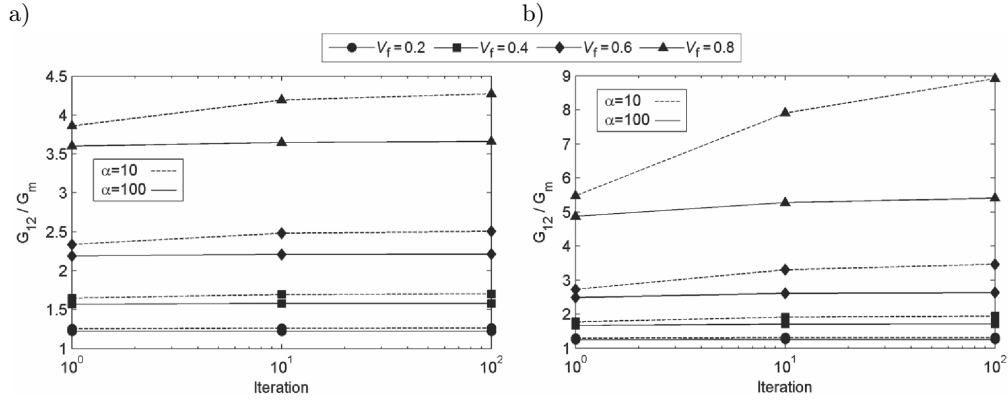


FIG. 5. Convergence trend of normalized effective in-plane shear modulus for different values of filler volume fraction and aspect ratio: a)  $E_f/E_m = 10$ , b)  $E_f/E_m = 100$ .

that the number of iterations required for convergence is directly related to the degree of reinforcement and elastic moduli ratio, but inversely to the filler aspect ratio.

#### 4. Micromechanical modeling of intercalated polymer/clay nanocomposite

##### 4.1. Structure of intercalated nanoclay

The hierarchical structure of the intercalated nanoclay is shown in Fig. 6 which is used as an effective continuum particle in most of the analytical/numerical micromechanical models [23–29, 34, 35]. This equivalent model is defined as a multi-layer stack containing  $N$  single silicate layers, each with effective thickness  $d_s$  and uniform inter-layer spacing  $d_{001}$ . Separating sheets are so-called gallery layers comprising both surfactants and polymer chains that have penetrated the inter-silicate layers during the synthesis process of nanocomposite. The overall particle thickness  $t$  can be related to the nanoclay structural parameters  $N$ ,  $d_{001}$ , and  $d_s$  as follows:

$$(4.1) \quad t = (N - 1)d_{001} + d_s.$$



FIG. 6. Schematic continuum representation for the hierarchical structure of intercalated nanoclay.

In order to use the Eshelby-based micromechanical models, the effective particle is considered as a high-aspect-ratio ellipsoidal inclusion (ideally known as penny shape) described by Eq. (3.1) as follows:  $a_1 = a_2 \gg a_3$ .

According to the hierarchical structure of intercalated nanoclay, the volume fraction of effective intercalated particles could be obtained using the following equation:

$$(4.2) \quad V_f = V_f' \left( 1 + \frac{N-1}{N} \frac{d_{001}}{d_s} \right),$$

where  $V_f'$  is the total volume fraction of filler in the nanocomposite. Since the filler content in experimental studies is specified based on the ratio of its weight to total composite weight, it is necessary to relate the weight fraction of filler  $W_f$  to its volume fraction through

$$(4.3) \quad V_f' = \frac{W_f/\rho_f}{W_f/\rho_f + (1-W_f)/\rho_m},$$

where  $\rho_m$  and  $\rho_f$  are the matrix and filler densities, respectively.

#### 4.2. Mechanical properties of the effective clay particle

The elastic constants of the effective particle could be obtained using the following equilibrium and continuity conditions:

$$(4.4) \quad \begin{aligned} \sigma_{ij}^{\text{avg}} &= V_g \sigma_{ij}^g + V_s \sigma_{ij}^s, & \varepsilon_{ij}^g &= \varepsilon_{ij}^s & \text{for } i, j = 1, 2, \\ \varepsilon_{3i}^{\text{avg}} &= V_g \varepsilon_{3i}^g + V_s \varepsilon_{3i}^s, & \sigma_{3i}^g &= \sigma_{3i}^s & \text{for } i = 1, 2, 3, \end{aligned}$$

where  $\sigma_{ij}^{\text{avg}}$  and  $\varepsilon_{ij}^{\text{avg}}$  are the average stress and strain components in the nanoclay representative element, and  $V_s$  and  $V_g$  are volume fractions of the silicate and gallery layers in the intercalated nanoclay, respectively. Superscripts  $s$  and  $g$  refer to silicate layers and intra-gallery, respectively.

Assuming orthotropic properties for both, silicate layers and intra-gallery, average stresses and strains in each layer as well as the effective particle can be related by Hook's law:  $\boldsymbol{\sigma} = \mathbf{C}\boldsymbol{\varepsilon}$  where

$$(4.5) \quad \mathbf{C}^{-1} = \begin{bmatrix} 1/E_1 & -\nu_{21}'E_2 & -\nu_{31}'E_3 & 0 & 0 & 0 \\ -\nu_{12}'E_1 & 1/E_2 & -\nu_{32}'E_3 & 0 & 0 & 0 \\ -\nu_{13}'E_1 & -\nu_{23}'E_2 & 1/E_3 & 0 & 0 & 0 \\ 0 & 0 & 0 & 1/G_{13} & 0 & 0 \\ 0 & 0 & 0 & 0 & 1/G_{23} & 0 \\ 0 & 0 & 0 & 0 & 0 & 1/G_{12} \end{bmatrix}.$$

Substituting Hook's law into Eq. (4.4) results in the stiffness tensor of the effective particle with orthotropic symmetry which could be written in Voigt's notation as:

$$(4.6) \quad \mathbf{C} = \begin{bmatrix} C_{11} & C_{12} & C_{13} & 0 & 0 & 0 \\ C_{12} & C_{22} & C_{23} & 0 & 0 & 0 \\ C_{13} & C_{23} & C_{33} & 0 & 0 & 0 \\ 0 & 0 & 0 & C_{44} & 0 & 0 \\ 0 & 0 & 0 & 0 & C_{55} & 0 \\ 0 & 0 & 0 & 0 & 0 & C_{66} \end{bmatrix}.$$

The elements of fourth-order elasticity tensor  $L$  are related to the components of stiffness tensor through

$$(4.7) \quad L_{ijkl} = C_{ik}\delta_{IJ}\delta_{KL} + C_{(3+m)k}\delta_{KL}(1 - \delta_{IJ}) + C_{i(3+n)}\delta_{IJ}(1 - \delta_{KL}) \\ + C_{(3+m)(3+n)}(1 - \delta_{IJ})(1 - \delta_{KL}),$$

where  $m \neq i, j$  and  $n \neq k, l$  for  $i, j, k, l, m, n = 1, 2, 3$ .

Upper case indices in above equation take the same numbers as the corresponding lower case ones, but are not summed with them.

## 5. Results and discussion

The results of present method are compared with the experimental data given by WEON and SUE [36] for a nylon-6/clay nanocomposite with distribution of clay platelet aspect ratio and orientation.

### 5.1. Filler aspect ratio and orientation

WEON and SUE [36] have altered the aspect ratio and orientation of the clay nanoparticles using a large-scale simple shear process, called equal channel angular extrusion (ECAE) [37, 38]. They categorized the samples before and after ECAE as follow: reference, received a single ECAE pass (A1) and received two ECAE passes with a 180° rotation of specimen between the passes (C2). They applied a semi-automated image analysis technique to quantify the effect of ECAE on morphological properties of nanoparticles and found that the modulus, strength, and heat distortion temperature of nanocomposites would increase with the increase of the clay aspect ratio and degree of orientation. Figures 7a and 7b of [36] illustrate the statistical distribution of the nanoclay platelet aspect ratio and degree of orientation for samples of the reference, A1 and C2 nanocomposites, respectively.

To use illustrated data, some of the most common density functions (i.e., normal, log-normal, exponential, and weibull) are examined to see which could better reproduces data according to density distribution, range of variation, and the values of mean and standard deviation observed in these figures.

Statistical distribution of the nanoclay platelet aspect ratio  $\alpha$  can be best expressed using the log-normal probability density function (pdf) below:

$$(5.1) \quad \text{pdf}(\alpha) = \frac{e^{-(\ln(\alpha)-\mu)^2/2\sigma^2}}{\alpha\sigma\sqrt{2\pi}},$$

where  $\mu$  and  $\sigma$  are mean value and standard deviation of platelet aspect ratio.

Also, statistical distribution of the degree of platelet orientation  $\theta$  could be represented by the Weibull density function defined as

$$(5.2) \quad \text{pdf}(\theta) = \frac{\kappa\left(\frac{\theta}{\lambda}\right)^{\kappa-1} e^{-(\theta/\lambda)^\kappa}}{\lambda},$$

where  $\lambda$  and  $\kappa$  are related to mean value and standard deviation via the following equations:

$$(5.3) \quad \mu = \lambda\Gamma\left(1 + \frac{1}{k}\right), \quad \sigma = \lambda\sqrt{\Gamma\left(1 + \frac{2}{k}\right) - \Gamma\left(1 + \frac{1}{k}\right)^2},$$

where  $\Gamma$  is the gamma function defined by  $\Gamma(x) = \int_0^\infty s^{x-1}e^{-s}ds$ .

Values of the statistical parameters are listed in Table 1. Probability distribution diagrams of nanoclay platelet aspect ratio and degree of orientation are drawn in Figs. 7a and 7b, based on the values of Table 1.

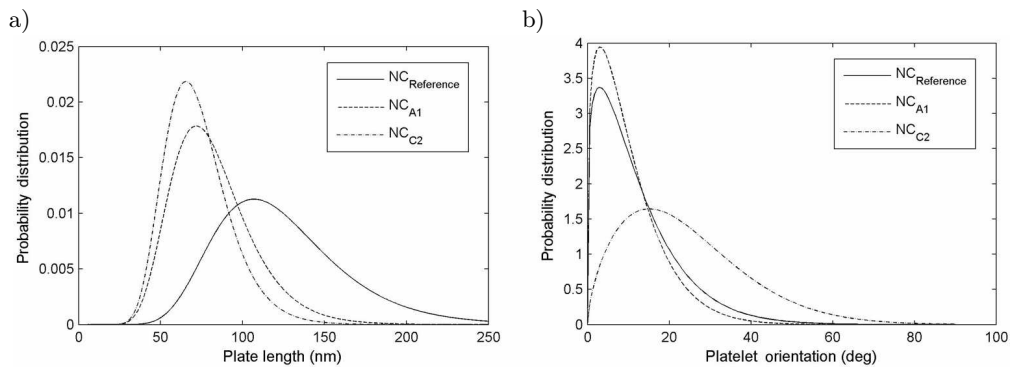


FIG. 7. Probability distribution diagrams of the annealed nanocomposites: a) platelet aspect ratio, b) platelet degree of orientation.

**Table 1. Statistical parameters corresponding to probability distribution of clay aspect ratio  $\alpha$  and orientation  $\theta$  for different samples tested by WEON and SUE [36].**

Sample	Aspect ratio (log-normal)		Orientation (weibull)	
	$\mu$	$\sigma$	$\kappa$	$\lambda$
Reference	132	33	1.205	0.223
A1	87	26	1.717	0.196
C2	78	21	1.642	0.468

### 5.2. Mechanical properties of a fully exfoliated nylon-6/clay nanocomposite

The material and structural properties of constituents of the nanocomposite samples produced by WEON and SUE [36] are listed in Table 2. The discretized distribution of filler orientation and aspect ratio could be obtained by dividing the area under the pdf curves into equal areas. The predicted elastic modulus is compared with the experimental data in Table 3 which shows a good agreement

**Table 2. Properties of the constituents of nanocomposite samples tested by WEON and SUE [36].**

$E_{\text{nylon}}$ (GPa)	$E_{\text{silicate}}$ (GPa)	$\nu_{\text{nylon}}$	$\nu_{\text{silicate}}$	$\rho_{\text{nylon}}$ (g/cm <sup>3</sup> )	$\rho_{\text{silicate}}$ (g/cm <sup>3</sup> )	$d_s$ (nm)	$N$	$W_f$
3.14	400	0.35	0.2	1.14	2.6 <sup>[34]</sup>	0.94	1	0.02

**Table 3. Predicted values of elastic moduli of nanocomposite samples tested by WEON and SUE [36].**

Sample	Study	Number of distributed angles ( $\theta$ )	Number of distributed values of aspect ratio ( $\alpha$ )	$\bar{E}_1/E_m$
Reference	WEON and SUE [36] present	5	5	1.487
		10	10	1.425
		10	10	1.439
		15	15	1.442
A1	WEON and SUE [36] present	5	5	1.302
		10	10	1.354
		15	15	1.363
C2	WEON and SUE [36] present	5	5	1.367
		10	10	1.210
		10	10	1.237
		15	15	1.236
				1.235

of the results. It is noticeable that the results are based on the assumption that the intra-gallery material has the same properties as that of the polymeric matrix.

## 6. Conclusion

An iterative process of micromechanical homogenization is proposed in this paper in order to characterize the mechanical behavior of nanoclay composites. This process is based on successively introducing a small fraction of heterogeneities until reaching the final reinforcement's volume fraction. The main feature of the present method is the possibility to define various kinds of inhomogeneity with different dimensional, micro-structural and mechanical properties within the matrix. Furthermore, any probability density function could be defined for the distribution of dimensions and orientations of filler particles.

As was shown in the literature, since the filler volume fraction at each iteration is small, all explicit homogenizations converge to the same prediction for the effective behavior, regardless of the filler volume fraction or the contrast between phases. Therefore, Mori–Tanaka's method was chosen as one of the most authentic micromechanical models used to predict the mechanical properties of composites and nanocomposites. Applying the iterative process for a unidirectional particulate composite revealed a significant difference from non-iterative approach especially for high volume fraction of filler component. It was also concluded that the number of iterations needed to obtain the convergence depends on the filler volume fraction and aspect ratio as well as the contrasts in the properties of the composite constituents.

The proposed approach is then applied for modeling nylon-6/clay nanocomposite taking into account the hierarchical structure of intercalated nanoclay and the probability distribution of aspect ratio and orientation of effective particles which shows a good agreement in comparison with available experimental data.

## References

1. Q.H. ZENGA, A.B. YUA, G.Q. LU, *Multiscale modeling and simulation of polymer nanocomposites*, Prog. Polym. Sci., **33**, 191–269, 2008.
2. J. GHANBARI, R. NAGHDABADI, *Hierarchical Multiscale Modeling of Nanotube-Reinforced Polymer Composites*, Int. J. Multiscale Comput. Eng., **7**, 395–408, 2009.
3. M. WANG, N. PAN, *Elastic property of multiphase composites with random microstructures*, J. Comput. Phys., **228**, 5978–5988, 2009.
4. J. PTASZNY, P. FEDELIŃSKI, *Numerical homogenization of polymer/clay nanocomposites by the boundary element method*, Arch. Mech., **63**, 517–532, 2011.

5. YU.I. DIMITRIENKO, A.P. SOKOLOV, *Numerical modeling of composites with multiscale microstructure*, Bulletin of the Russian Academy of Sciences: Physics, **75**, 1457–1461, 2011.
6. R.D. PENG, H.W. ZHOUA, H.W. WANGB, L. MISHNAEVSKY, *Modeling of nano-reinforced polymer composites: Microstructure effect on Young's modulus*, Comput. Mat. Sci., **60**, 19–31, 2012.
7. Q. LI, X.X. YANG, *Numerical Simulation for Mechanical Behavior of Carbon Black Filler Particle Reinforced Rubber Matrix Composites*, Appl. Mech. Mat., **137**, 1–6, 2012.
8. J.D. ESHELBY, *The determination of the elastic field of an ellipsoidal inclusion and related problems*, Proceeding of the Royal Society London A, **241**, 376–396, 1957.
9. R.M. CHRISTENSEN, *Mechanics of Composite Materials*, Dover Publications, 2005.
10. J. ABOUDI, *Mechanics of Composite Materials: A Unified Micromechanical Approach*, Elsevier Science Publishers Editor, B.V., Amsterdam 1991.
11. T. MORI, K. TANAKA, *Average stress in matrix and average elastic energy of materials with misfitting inclusions*, Acta Metall., **21**, 571–574, 1973.
12. E. HERVE, A. ZAOUI, *N-layered inclusion-based micromechanical modeling*, Int. J. Eng. Sci., **31**, 1–10, 1993.
13. M. BORNERT, C. STOLZ, A. ZAOUI, *Morphologically representative pattern-based bounding in elasticity*, J. Mech. Phys. Solids, **44**, 307–331, 1996.
14. A.N. NORRIS, *A differential schema for the effective moduli of composites*, Mech. Mater., **4**, 1–16, 1985.
15. R.W. ZIMMERMAN, *Elastic moduli of a solid containing spherical inclusions*, Mech. Mater., **12**, 17–24, 1991.
16. B. BUDIANSKY, *On the elastic moduli of some heterogeneous materials*, J. Mech. Phys. Solids, **13**, 223–227, 1965.
17. N. PHAN-THIEN, D.C. PHAM, *Differential multiphase models for polydispersed suspensions and particulate solids*, J. Non-Newtonian Fluid Mech., **72**, 305–318, 1997.
18. L. BARDELLA, F. GENNA, *On the elastic behavior of syntactic foams*, Int. J. Solids Struct., **38**, 7235–7260, 2000.
19. Y. KOJIMA, Y. USUKI, M. KAWASUMI, A. OKADA, Y. FUKUSHIMA, T. KURAUCHI, O. KAMIGAITO, *Mechanical properties of nylon 6-clay hybrid*, J. Mater. Res., **8**, 1185–1189, 1993.
20. J.S. SHELLEY, P.T. MATHER, K.L. DEVRIES, *Reinforcement and environmental degradation of nylon-6/clay nanocomposites*, Polymer, **42**, 5849–5858, 2001.
21. D.A. BRUNE, J. BICERANO, *Micromechanics of nanocomposites: comparison of tensile and compressive elastic moduli, and prediction of effects of incomplete exfoliation and imperfect alignment on modulus*, Polymer, **43**, 369–387, 2002.
22. J.C. HALPIN, J.L. KARDOS, *The Halpin-Tsai Equations: A Review*, Polym. Eng. Sci., **16**, 344–352, 1976.
23. J.-J. LUO, I.M. DANIEL, *Characterization and modeling of mechanical behavior of polymer/clay nanocomposites*. Compos. Sci. Technol., **63**, 1607–1616, 2003.

24. K. ANOUKOU, F. ZAÏRI, M. NAÏT-ABDELAZIZ, A. ZAOUÏ, T. MESSEGER, J.M. GLOAGUEN, *On the overall elastic moduli of polymer-clay nanocomposite materials using a self-consistent approach. Part I: Theory*, Compos. Sci. Technol., **71**, 197–205, 2011.
25. A. MESBAH, F. ZAÏRI, S. BOUTALEB, J. M. GLOAGUEN, M. NAÏT-ABDELAZIZ, S. XIE, T. BOUKHAROUBA, J. M. LEFEBVRE, *Experimental Characterization and Modeling Stiffness of Polymer/Clay Nanocomposites within a Hierarchical, Multiscale Framework*, J. Appl. Polym. Sci., **114**, 3274–3291, 2009.
26. F. ZAÏRI, J.M. GLOAGUEN, M. NAÏT-ABDELAZIZ, A. MESBAH, J.M. LEFEBVRE, *Study of the effect of size and clay structural parameters on the yield and post-yield response of polymer/clay nanocomposites via a multiscale micromechanical modeling*, Acta Mater., **59**, 3851–3863, 2011.
27. G.I. ANTHOULIS, E. KONTOU, *Micromechanical behaviour of particulate polymer nanocomposites*, Polymer, **49**, 1934–1942, 2008.
28. B. BUDIANSKY, T.Y. WU, *Theoretical prediction of plastic strains of polycrystals*, [in:] Proceedings of the 4th US National Congress of Applied Mechanics, 1175–1185, 1962.
29. J. WANG, R. PYRZ, *Prediction of the overall moduli of layered silicate-reinforced nanocomposites-part I: basic theory and formulas*, Compos. Sci. Technol., **64**, 925–934, 2004.
30. R. ZOUARI, A. BENHAMIDA, H. DUMONTET, *A micromechanical iterative approach for the behavior of polydispersed composites*, Int. J. Solids Struct., **45**, 3139–3152, 2008.
31. R. HILL, *A self-consistent mechanics of composite materials*, J. Mech. Phys. Solids, **13**, 213–222, 1965.
32. Z. HASHIN, S. SHTRIKMAN, *A variational approach to the theory of the elastic behavior of multiphase materials*, J. Mech. Phys. Solids, **11**, 127–140, 1963.
33. J. QU, M. CHERKAOUÏ, *Fundamentals of micromechanics of solids*, Wiley, Hoboken, New Jersey, 2006.
34. N. SHENG, M.C. BOYCE, D.M. PARKS, G.C. RUTLEDGE, J.I. ABES, R.E. COHEN, *Multiscale micromechanical modeling of polymer/clay nanocomposites and the effective clay particle*, Polymer, **45**, 487–506, 2004.
35. A. ZARE-SHAHABADI, A. SHOKUH FAR, S. EBRAHIMI-NEJAD, M. ARJMAND, M. TERMEH, *Modeling the stiffness of polymer/layered silicate nanocomposites: More accurate predictions with consideration of exfoliation ratio as a function of filler content*, Polym. Test., **30**, 408–414, 2011.
36. J.-I. WEON, H.-J. SUE, *Effects of clay orientation and aspect ratio on mechanical behavior of nylon-6 nanocomposite*, Polymer, **46**, 6325–6334, 2005.
37. T.S. CREASY, Y.S. KANG, *Fiber orientation during equal channel angular extrusion of short fiber reinforced thermoplastics*, J. Thermoplast. Compos. Mater., **17**, 205–227, 2004.
38. Z.Y. XIA, *Processing-structure-property relationships in oriented polymers*, Ph.D. Dissertation, Texas A&M University, Department of Mechanical Engineering, 2001.

Received January 17, 2012; revised version October 14, 2012.